Chalcogenide Letters Vol. 11, No. 10, October 2014, p. 509 - 517

INVESTIGATIONS ON PHYSICAL PROPERTIES OF NANOSTRUCTURED ZnTe THIN FILMS PREPARED BY DC REACTIVE MAGNETRON SPUTTERING

B. RAJESH KUMAR*, B. HYMAVATHI[a], T. SUBBA RAO[a]
Department of Physics, GITAM Institute of Technology, GITAM University, Visakhapatnam - 530 045, A.P, India.
[a]Materials Research Lab, Department of Physics, Sri Krishnadevaraya University, Anantapuramu - 515 003, A.P, India.

Nanostructured ZnTe thin films were deposited on glass substrates by DC reactive magnetron sputtering technique. The depositions were carried out by varying the substrate temperature from RT to 350 ^{o}C. X-ray diffraction patterns shows that ZnTe thin films are polycrystalline in nature with cubic structure showing preferred orientation in (1 1 1) direction. The crystallite size and the intensity of XRD peaks increases with the increase of substrate temperature which implies better crystallinity takes place at higher temperature. The electrical resistivity of the films decreases with the increase of substrate temperature. The optical band gap values of ZnTe thin films are varied from 2.35 to 2.61 eV with the increase of substrate temperature and refractive index of the films are decreased from 2.90 to 2.66 with the increase of substrate temperature.

(Received September 6, 2014; Accepted October 13, 2014)

Keywords: Thin films, DC reactive magnetron sputtering, Structural properties, Optical properties

1. Introduction

II-VI semiconductors have attracted many researchers because of their possible applications in the fabrication of solar cells, light emitting diodes (LEDs), photodiodes and many other optoelectronic devices. Zinc Telluride (ZnTe) is one of the important members of II-VI compound semiconducting material having electrical and optical properties suitable for the fabrication of various optoelectronic devices [1]. It has a wide and direct bandgap of 2.26 eV (at room temperature) which is the pure green region of the electromagnetic spectra. This direct band gap makes it a potential candidate for the fabrication of pure green LEDs. Because of its high electro-optic coefficient, ZnTe promises to be useful in the production and detection of terahertz (THz) radiation. ZnTe possess a cubic zinc blende type structure with lattice constant a = 0.6103 nm. Usually, it is a material of high absorption coefficient and shows p-type nature [2].

Many fabrication techniques like thermal evaporation [3], e-beam evaporation [4], molecular- beam epitaxy (MBE) [5], sputtering [6], metal organic chemical vapour deposition (MOCVD) [7] etc. have been attempted for depositing ZnTe thin films. Among these DC reactive magnetron sputtering is the most promising technique because of its high deposition rate, large area scalability, and easy preparation of a large size as well as a high conductivity and visible transmittance [8]. The present work is focused on the influence of substrate temperature on structural, electrical and optical properties of ZnTe thin films. This paper reports the first observation of ZnTe thin films sputtered by using individual metallic targets of Zn and Te.

* Corresponding author: rajphyind@gmail.com

2. Experimental details

In the present work ZnTe thin films were deposited on glass substrates by using individual metallic targets of Zn and Te. The thin films were deposited by varying substrate temperatures from RT (= 30 ^{o}C) to 350 ^{o}C. The sputtering targets of size 2 inch diameter and 4 mm thickness of Zn (99.99% purity) and Te (99.99% purity) were used in the present study. Pure argon used as sputter gas was admitted into the chamber through mass flow controller (Model GFC 17, Aalborg, Germany). The base pressure in the chamber was 2.4 x 10^{-6} Torr and the distance between target and substrate was set to 60 mm. Deposition was carried out at a working pressure of 3 mTorr after pre-sputtering with argon for 10 min. The sputtering power was maintained at 105 W for Zn and 80 W for Te during deposition. Film thickness was measured by Talysurf thickness profilometer. The resulting thickness of the films is ~ 300 - 350 nm. X-ray diffraction (XRD) patterns of the films were recorded with the help of Philips (PW 1830) X-ray diffractometer using CuKα radiation. The tube was operated at 30 KV, 20 mA with the scanning speed of 0.03(2θ)/sec. Surface topography of the films have been studied using AFM (Park XE-100: Atomic Force Microscopy). The resistivity of the films (ρ) was measured using the four-point probe method. Optical transmittance of the films was recorded as a function of wavelength in the range of 300 – 1200 nm using JASCO Model V-670 UV-Vis-NIR spectro-photometer (Japan).

3. Results and discussion

X-ray diffraction patterns of ZnTe thin films deposited on glass substrates are shown in Fig. 1. A strong peak is observed around at 2θ = 25.48^{o} which corresponds to preferred orientation along (1 1 1) plane of cubic phase. It is good agreement with the standard JCPDS-ICDD (01-0582) data of ZnTe.The intensity of the peak (1 1 1) increases and the full width at half maximum (FWHM) of the films decreases with the increase of substrate temperature from RT (= 30 ^{o}C) to 350 ^{o}C. The increase in peak intensity and decrease of FWHM is due to the improvement in the crystallinity of the films at different substrate temperatures.

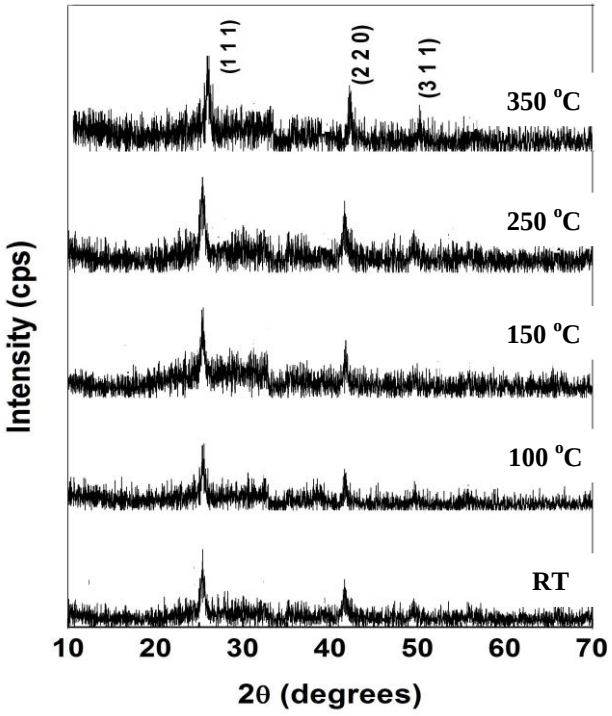

Fig. 1 XRD patterns of ZnTe thin films deposited at different substrate temperatures

The lattice constant 'a' for the cubic phase structure is determined by the relation

$$a = d.\sqrt{h^2+k^2+l^2} \qquad \text{nm}$$

The lattice constant values of ZnTe thin films decreases from 0.6048 to 0.6002 nm with the increase of substrate temperature. The average crystallite size (D) of the films is estimated from Scherrer formula [9]. It is observed that the crystallite size of the films increases with increased substrate temperature and reached a maximum value of 33 nm at substrate temperature of 350 ^{o}C. Due to the increase of crystallite size with substrate temperature, the defect in the lattice is decreased, which in turn reduces the stress, internal microstrain and dislocation density [10, 11].

The origin of the strain is related to the lattice misfit which in turn depends on the deposition conditions. The microstrain (ε) developed in the ZnTe films was calculated by using the relation

$$\varepsilon = \frac{\beta\cos\theta}{4} \qquad \text{lin}^{-2}.\text{m}^{-4}$$

where β is the full width at half maximum of (1 1 1) peak.

A dislocation is an imperfection in a crystal associated with the misregistry of the lattice in one part of the crystal with that in another part. Unlike vacancies and interstitial atoms, dislocations are not equilibrium imperfections, i.e. thermodynamic considerations are insufficient to account for their existence in the observed densities. In fact, the growth mechanism involving dislocation is a matter of importance. In the present study, the dislocation density for cubic ZnTe thin films is estimated from Williamson and Smallman's formula [12]

$$\delta = \frac{n}{D^2} \qquad \text{lin.m}^{-2}$$

where n is a factor, which when equal to unity gives the minimum dislocation density and D is the average crystallite size.

The number of crystallites per unit area (N) is determined from the thickness (t) of the films using the relation

$$N = \frac{t}{D^3} \qquad \text{m}^{-2}$$

The decrease of micro stain (ε) and dislocation density (δ) at higher substrate temperatures may be due to the movement of interstitial Zn atoms from inside the crystallites to its grain boundary which dissipate leading to reduction in the concentration of lattice imperfections. The microstructural parameters of ZnTe thin films deposited at different substrate temperatures are given in Table 1. The results obtained are in good agreement with the previous reported literature [13].

Table 1. Structural parameters of ZnTe thin films

S.No	Substrate temperature (^{o}C)	d -spacing (nm)	Lattice constant, a (nm)	Crystallite size, D (nm)	Strain, ε x 10^{3} (lin^{-2}.m$^{-4)}$	Dislocation density, δ x 10^{15} (lin.m^{-2})	Number of crystallites per unit area, N (m^{-2})
1	RT	0.3492	0.6048	14	0.203	5.10	1.27 x 10^{19}
2	100	0.3487	0.6040	16	0.198	3.91	0.85 x 10^{19}
3	150	0.3477	0.6023	22	0.182	2.07	0.32 x 10^{19}
4	250	0.3471	0.6012	28	0.176	1.28	0.16 x 10^{19}
5	350	0.3465	0.6002	33	0.166	0.91	0.97 x 10^{18}

Surface topography of the films deposited at different substrate temperatures was studied by atomic force microscope (AFM). AFM images are utilized for measuring the surface roughness of the films. Surface roughness is a measure of the texture of the films. To characterize an optical coating, the root mean square (RMS) roughness is normally used. The RMS roughness not only describes the light scattering but also gives an idea about the quality of the surface under investigation. Average roughness (r_{avg}) is defined as the mean absolute values of the profile heights measured from a mean plane averaged over the sampling area (amplitude type), while the root mean square (RMS) roughness (r_{RMS}) is the standard deviation of the surface from the mean plane over the sampling area[14,15]. The average roughness (r_{avg}) and RMS roughness (r_{RMS}) are determined from the relations:

$$r_{avg} = \frac{1}{N}\sum_{i=1}^{N}\left|H_i\right|$$

$$r_{RMS} = \sqrt{\frac{\sum_{i=1}^{N}\left|H_i^2\right|}{N}}$$

where N is the number of obtained surface points and H_i is the height of the i^{th} element obtained from AFM analysis. Surface topography of the ZnTe thin film deposited at substrate temperature of 350 ^oC is shown in Fig. 2. It can be observed that the microstructural features of the sample are characterized by high-density columnar structure.

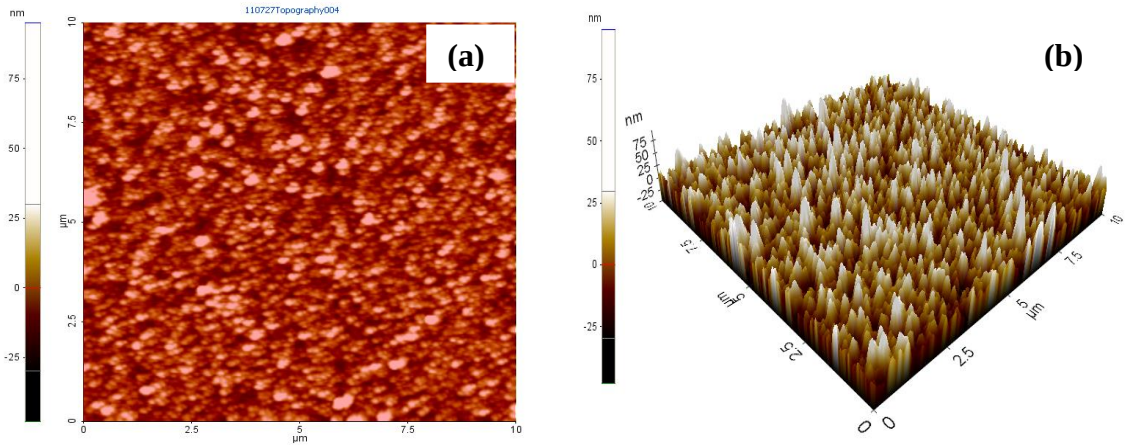

Fig. 2 (a) Two dimensional (2D) and (b) Three dimensional (3D) topographic AFM images of ZnTe thin film deposited at 350 ^oC

The grain size distribution image for ZnTe thin film deposited at substrate temperature of 350 ^oC is shown in Fig. 3. The effects of grain size evolution during film deposition are evident on the variation of crystallographic texture and the RMS roughness. Although grain growth is still occurring, this roughening is due to shadowing of the arriving atomic flux leading to hillock growth and the increase in ridge height. Software-based image processing of AFM data can generate quantitative information from individual grains or group of grains. Statistics on groups of particles can also be measured through image analysis and data processing. Quantitative analysis which gives the statistical information on surface area, volume, length and perimeter distributions of nanostructured ZnTe thin film deposited at substrate temperature of 350 ^oC is shown in Fig. 4.

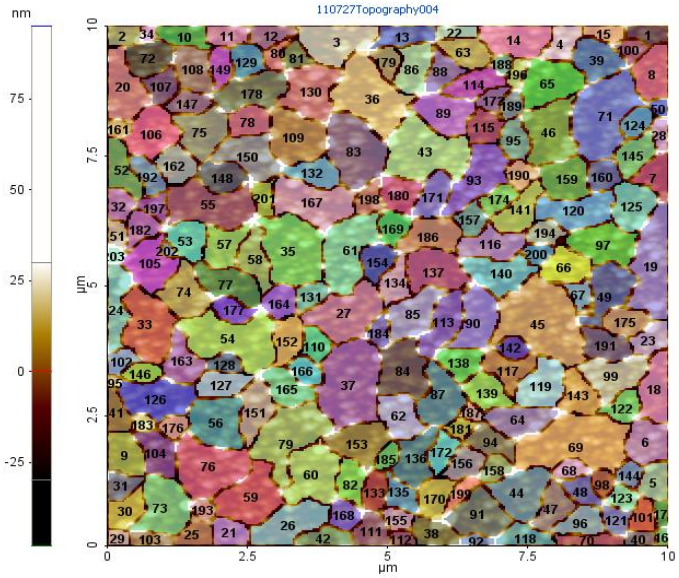

Fig.3 Grain size distribution image for ZnTe thin film deposited at 350 ^{o}C

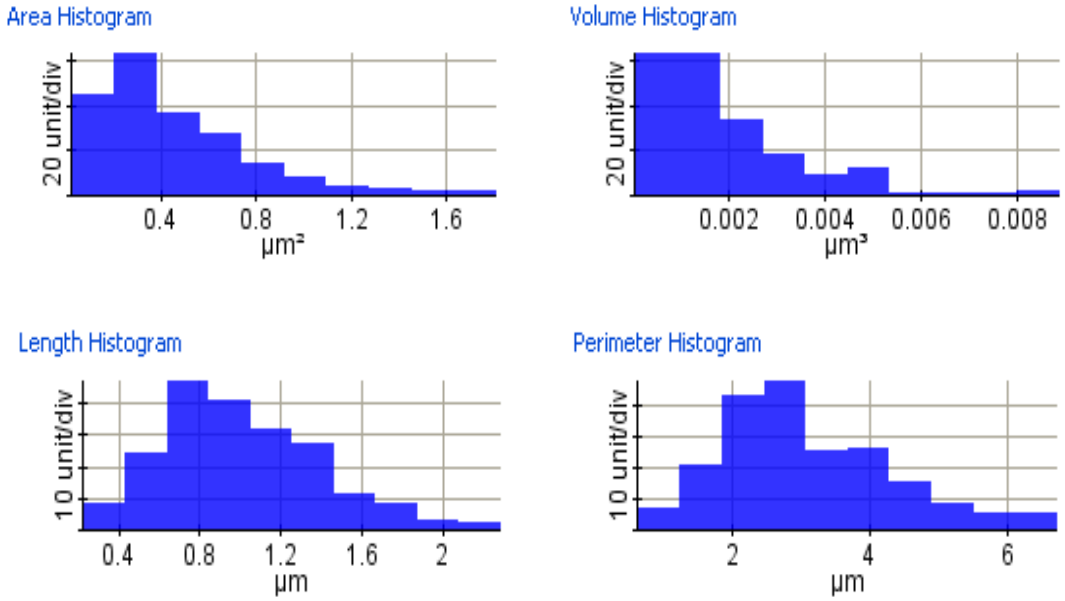

Fig. 4 Quantitative analysis of ZnTe thin film deposited at substrate temperature of 350 ^{o}C

Composition of the films was estimated from energy dispersive analysis of X-rays (EDAX). The relative compositions for ZnTe films deposited from RT (= 30 ^{o}C) to 350 ^{o}C are in an atomic ratio of Zn/Te are 50.25/49.75%, 51.50/48.50%, 51.70/48.30%, 51.95/48.05% and 52.20/47.80%. The stoichiometric deviation results the high conductivity of these films.

Four probe method was employed to determine the resistivity of ZnTe thin films. The resistivity of the films decreases with the increase of substrate temperature from RT to 350 ^{o}C. The variation of electrical conductivity (σ) of nanocrystalline ZnTe films with temperature indicates typical Arrhenius type of activation

$$\sigma = \sigma_o \exp\left(-\frac{\Delta E}{k_B T}\right)$$

where ΔE denotes the thermal activation energy of electrical conduction, σ_o represents a parameter depending on the semiconductor nature and k_B is the Boltzmann's constant. It is

observed that the conductivity changes continuously with temperature. This indicates that the conduction mechanism is due to thermally assisted tunneling of charge carriers in the localized states in band tails. The plot of ln σ versus 1000/T consists of two linear parts at two different temperature ranges, the first region extends between 303 and 388 K (lower temperature region) and the second region between 388 and 573 K(higher temperature region) indicating two types of conduction mechanisms through thermally activated process(shown in Fig. 5). The activation energy values are evaluated from the slope of ln σ versus 1000/T (K^{-1}) plot in the lower and higher temperature range. The activation energy values of ZnTe thin films decreases with the increase of substrate temperature as given in Table 2. The low values of ΔE obtained at lower temperature indicates that hopping of the carriers between the localized states within or outside the Coulomb gap may be the dominant transport mechanism in these films. This result indicates that the conduction is due to thermally assisted tunneling of charge carriers in the localized states in band tails.

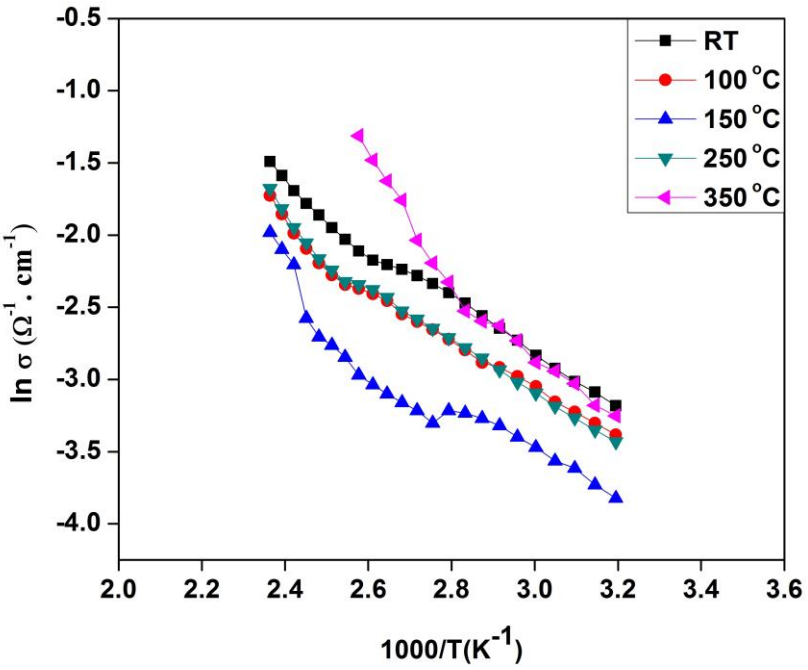

Fig. 5 Temperature dependence of electrical conductivity for ZnTe thin films

Table 2. Electrical resistivity and activation energy values of ZnTe thin films deposited at different substrate temperatures

S.No	Substrate Temperature (^oC)	Electrical resistivity, ρ (Ω.cm)	Activation energy ΔE (eV)	
			Region I	Region II
1	RT	2.46×10^6	0.34	0.68
2	100	1.08×10^6	0.31	0.64
3	150	0.84×10^6	0.28	0.52
4	250	0.62×10^6	0.24	0.46
5	350	0.49×10^6	0.22	0.40

Optical transmittance spectra of ZnTe thin films deposited on glass substrate at different substrate temperatures is shown in Fig. 6. The optical transmittance of the films increases with the increase of substrate temperature from RT to 350 ^{o}C. The optical band gap is calculated from the relationship between absorption coefficient and photon energy [16]:

$$(\alpha h\nu) = B(h\nu - E_g)^{1/2}$$

where α is the optical absorption coefficient, $h\nu$ is the photon energy, E_g is the optical band gap, and B is a constant. E_g values are determined from the intercept of extrapolated linear portion of $(\alpha h\nu)^2$ versus $h\nu$ curve to the photon energy axis. The shift observed at absorption edge towards lower photon energies for the heat treated layers could be attributed to the change in the grain size and the stoichiometry due to loss of Zn resulting formation of shallow acceptor levels [17, 18].

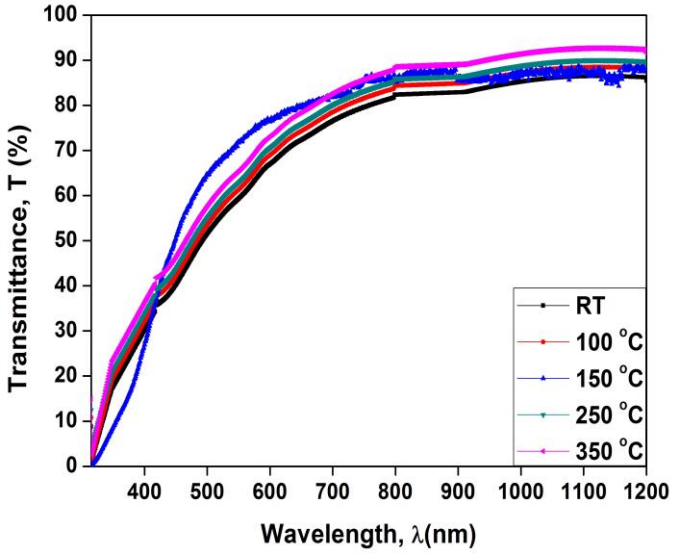

Fig. 6 Optical transmittance spectra for ZnTe thin films

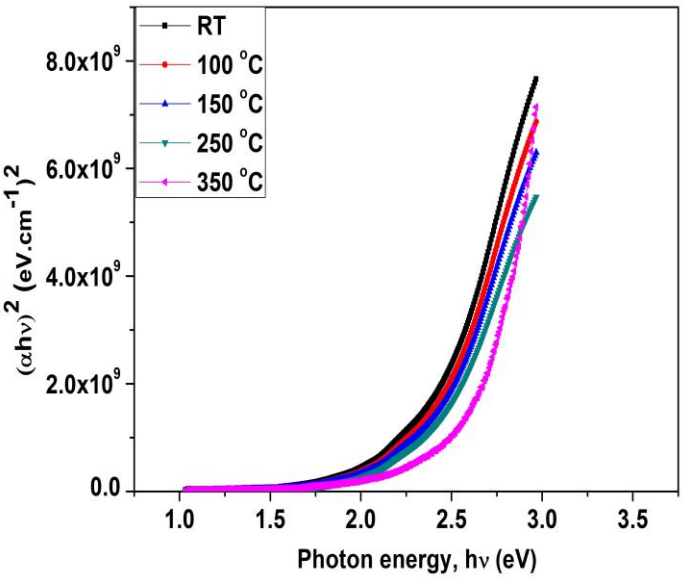

Fig. 7 Variation of $(\alpha h\nu)^2$ with photon energy ($h\nu$) for ZnTe thin films

Figure 7 shows the plot between $(\alpha h\nu)^2$ and photon energy ($h\nu$) for ZnTe thin films deposited at different substrate temperatures. The optical band gap of ZnTe thin films increases from 2.35 to 2.61 eV with the increase of substrate temperature from RT to 350 ^oC.

Similar results on the energy band gap have been observed for ZnTe thin films by using RF sputtering deposition technique [19]. Optical constants such as absorption coefficient (α), extinction coefficient (k) and refractive index (n) for ZnTe polycrystalline thin films are calculated from the equations reported in the previous literature [20]. Table 3 shows the optical parameters of ZnTe thin films deposited at different substrate temperatures. A high value of absorption coefficient (10^4 cm^{-1}) is observed for all the films. This behavior is a clear indication that the films are becoming highly transparent at long wavelengths. This suggests that the increase in transparency is likely to be originating from the observed decrease in extinction coefficient k with increasing substrate temperature. The refractive index of the films decreases with the increase of substrate temperature due to more stoichiometric and uniform. The stoichiometry and enhancement in crystallanity of the films at elevated substrate temperature consequences shift in optical band gap [21].

Table 3. Optical paramaters of ZnTe thin films deposited at different substrate temperatures

S.No	Substrate Temperature (^oC)	Absorption coefficient at 800 nm, α (cm^{-1})	Extinction coefficient at 800 nm, k	Optical band gap, E_g (eV)	Refractive index, n
1	RT	4.50×10^4	0.043	2.35	2.90
2	100	3.84×10^4	0.036	2.40	2.82
3	150	3.52×10^4	0.033	2.44	2.78
4	250	3.32×10^4	0.031	2.50	2.76
5	350	2.50×10^4	0.024	2.61	2.66

4. Conclusions

ZnTe thin films were deposited on glass substrate by DC reactive magnetron sputtering at different substrate temperatures. XRD studies reveal that the films are crystalline in nature and exhibit cubic structure with preferred orientation along the (1 1 1) plane. The decrease in the electrical resistivity with the increase of the substrate temperature is due to the improvement in the degree of crystallinity of the films as revealed by the XRD. The optical transmittance of the films increases with the increase of substrate temperature. The optical band gap of the films varies from 2.35 to 2.61 eV with the substrate temperature. The obtained results confirm that the nanostructured ZnTe thin films are excellent candidate for optoelectronic devices.

References

[1] M. Aven, J. Appl. Phys. **38**, 4421 (1967).
[2] M. Aven, B. Segall, Phys. Rev. **130**, 81 (1963).
[3] R. Chakrabarti, S. Ghosh, S. Chaudhuri, A. K. Pal, J. Phys. D: Appl. Phys. **32**, 1258 (1999).
[4] R. Islam, H. D. Banerjee, D. R. Rao, Thin Solid Films **266**, 215 (1995).
[5] Y. P. Chen, S. Sivananthan, J. P. Faurie, J. Electron. Mater. **22**, 951 (1993).
[6] A. Gupta, V. Parikh, A. D. Compaan, Sol. Energy Mater. Sol. Cells **90**, 2263 (2006).
[7] M. C. Nuss, D. W. Kisker, P. R. Smith,T. E. Harvey, Appl. Phys. Lett. **54**, 57 (1989).
[8] S.J. Jung, B.M. Koo, Y.H. Han, J.J.Lee, J.H. Joo, Surf. Coat. Technol. **200**, 862 (2005).
[9] B.D. Cullity, Elements of X-ray diffraction, Addition-Wesley, London (1959).
[10] N. El-Kadry, A. Aahour, S.A. Mohamoud, Thin Solid Films **269**,112 (1995).
[11] H.Y. Joo, H.J. Kim, J. Vac. Sci. Technol. A **17**, 862 (1999).

[12] C.K. De, N.K. Mishra, Indian J. Phys. **A 71**, 530 (1997).
[13] A.E. Merad, M.B. Kanoun, G. Merad, J. Cilat, H. Aourag, Mater. Chem. Phys. **92**, 333 (2005).
[14] E.S. Gadelmawla, M.M. Koura, T.M. Maksoud, I. M. Eleva, H.H. Soliman, J. Mater. Process. Technol. **123**, 133 (2002).
[15] M. Pelliccione, T.M. Lu, Evolution of thin film morphology: modelling and simulations, Springer, Berlin (2008).
[16] F.F.Yang, L. Fang, S.F. Zhang, K.J. Liao, G.B.Liu, J.X. Dong, L. Li, G.Z. Fu, J. Cryst. Growth **297**, 411 (2006).
[17] R.F.C. Farrow, G.R. Jones, G.M. Williams, I.M. Young, Appl. Phys. Lett. **39**, 954 (1981).
[18] D.H. Levi, H.R. Moutinho, F.S. Hasoon, B.M. Keyes, R.K. Ahrenkiel, M.Al-Jassim, L.L. Kazmerski, R.W. Birkmire, Sol. Energy Mater. Sol. Cells **41**, 381 (1996).
[19] H. Bellakhder, A. Outzourhit, E.L. Ameziane, Thin Solid Films 382 (2001) 30.
[20] B. Rajesh Kumar, T. Subba Rao, Chalcogen. Lett. **8**, 83 (2011).
[21] L.I. Maissel, R. Glang, Handbook of thin film technology, McGraw Hill, New York (1983).